

Electron-beam annealing of micro-sized objects and structures in SEM

K. V. Genkov*, G. G. Tsutsumanova, S. A. Hadjiiski, A. N. Tzonev, D. L. Lyutov, S. C. Russev

*Department of Solid State Physics and Microelectronics, Faculty of Physics,
St. Kliment Ohridski University of Sofia, 5 James Bourchier Blvd., BG-1164 Sofia, Bulgaria*

The heating effect of the focused electron beam in a Scanning Electron Microscope (SEM) opens up possibilities for annealing of micro-sized objects and structures. These possibilities are studied by investigating the heating effect under different conditions (beam power, spot size, etc) both by simulations and experiments. By reaching the melting point of the micro objects, it is shown that temperatures, sufficient for annealing, are achievable. Three setups are studied: heating via electron-beam, via tungsten heater and a combined setup.

Key words: SEM, electron beam heating, micro-scale annealing, zone melting

INTRODUCTION

The main purpose of this paper is to demonstrate that a scanning electron microscope (SEM) has the potential to be used as a tool for annealing of micro-sized objects.

SEM is a modern microscopy technique that uses a focused electron beam, scanning on the surface of the specimen. Various detectors analyze the electron-specimen interaction: back-scattered electrons (BSE), secondary electrons (SE), x-ray emission, cathodoluminescence (CL), emission of Auger electrons, etc [1–3]. Apart from all these effects, another consequence is heating of the specimen due to inelastic scattering [2, 4]. In fact, a major part of the energy of the primary electrons turns into heat. At higher beam currents, compared to the normal working conditions for imaging in SEM, the heating effect becomes more significant and could be sufficient for reaching a temperature of the specimen that is close to (and even beyond) its melting point. Further more, since the position of the beam can be precisely manipulated, it can be used for localized annealing of micro-sized objects and structures [5].

This method could be used for enhancing the crystalline structure of microcrystals, evaporating foreign particles, deposited on their surface, microwelding, etc. The production of near-perfect Ag/Au microcrystals is highly demanded in the field of plasmonics since any kind of defects act as scattering centers, leading to losses.

The applicability of SEM for thermal manipulation of micro-sized objects is demonstrated by simu-

lations that evaluate the temperature of the specimen under different conditions and by preliminary experiments where silver microparticles were melted.

SIMULATIONS

Preliminary data on the temperature across the volume of the electron-beam heated microparticle is obtained by computer simulations performed on COMSOL Multiphysics. The model consists of an Ag hexagonal microplate (same as the particles, used in the experiments) on top of a Si substrate.

For obtaining the thermal balance, the heat equation is solved [6]:

$$\frac{\partial T}{\partial t} = \frac{1}{\rho C_P} \nabla \cdot (k \nabla T) + \frac{q}{\rho C_P}, \quad (1)$$

where k stands for the material's conductivity and q is the density of the heat power (Wm^{-3} , positive values stand for heat sources while negative – for heat sinks).

The electron-beam heating is modeled as a volumetric heat source, shaped as a rectangular prism with width w , length l and depth h . Reasonable lengths of these dimensions are $w = l = 0.5 \mu\text{m}$ (the cross section depends on the field of view and therefore on the magnification) and $h = 200\text{--}300 \text{ nm}$ (equals the thickness of the microparticle).

The total power P_{beam} of the beam of accelerated electrons is

$$P_{\text{beam}} = eU \frac{dN_e}{dt} = IU, \quad (2)$$

where e is the electron charge, U – the accelerating voltage, $\frac{dN_e}{dt}$ is the flow of electrons and I – the beam current. A typical value for the accelerating voltage is $U = 30 \text{ kV}$ and the maximal beam current (measured by using a Faraday's cage specimen)

* To whom all correspondence should be sent:
kgenkov@uni-sofia.bg

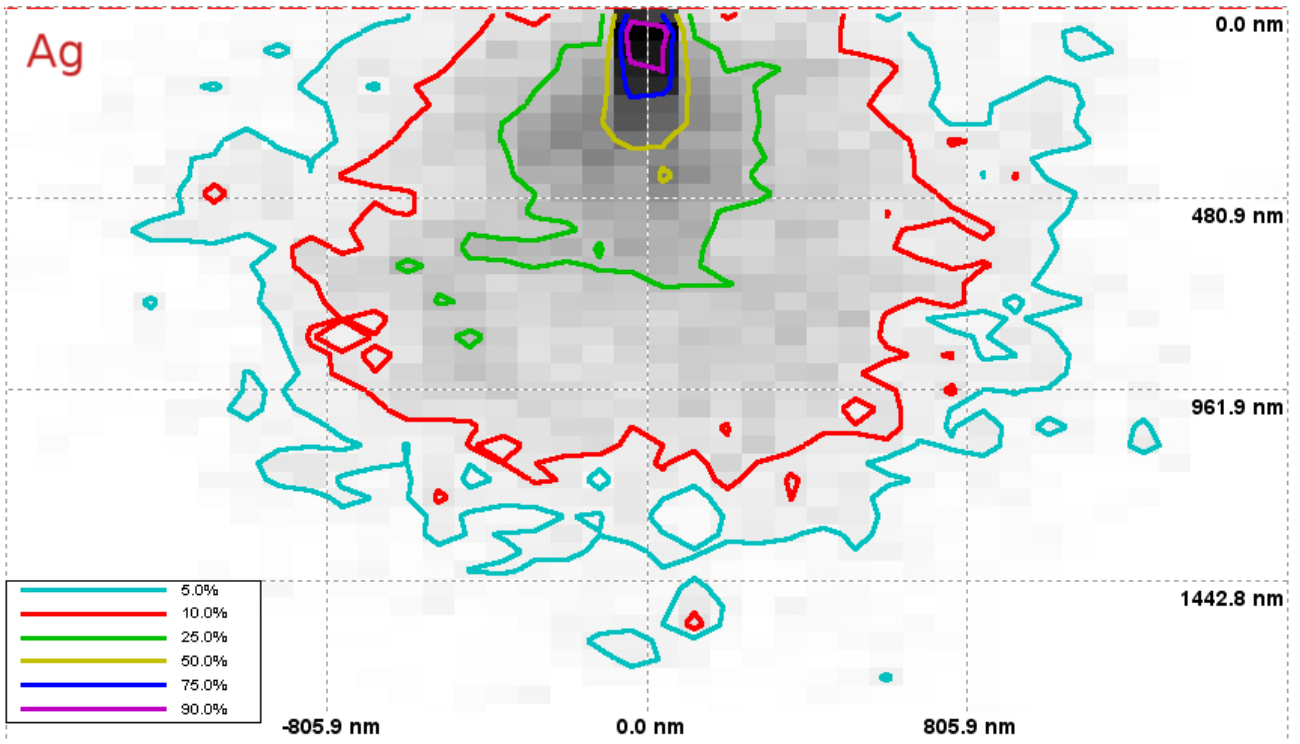


Fig. 1. Distribution of the dissipated energy in Ag. Each contour labeled as $X\%$ surrounds a region, in which $(100 - X)\%$ of the energy was dissipated. For example, inside the red contour $(100 - 10)\% = 90\%$ were dissipated.

Table 1. Boundary conditions of the simulations

Boundary	Condition
Top face of Ag hexagonal prism Side faces of Ag hexagonal prism	Gray body radiation
Interface between Ag and Si substrate	Thermal contact
Bottom face of Si substrate	Fixed at room temperature
Side faces of Si substrate Top face of Si substrate (excluding Ag-Si interface)	Thermally insulated

is $I_{\max} = 18.4 \mu\text{A}$ (by specifications, $I_{\max} = 300 \mu\text{A}$, see Table 2).

The heating power Q is less than the total power of the beam:

$$Q = cP_{\text{beam}}, \quad (3)$$

where $0 < c < 1$ is a coefficient that represents the portion of the energy of the primary beam that is transferred as heat in the area of interest and c depends on various parameters, for example the chemi-

cal composition of the specimen, its thickness, accelerating voltage, etc. A reasonable value $c = 0.5$ was obtained using the specialized software CASINO that performs Monte-Carlo simulations of the trajectories of the electrons in specimen [7] (Fig. 1).

Finally, assuming that the density of the heating power q is homogeneous across the heating region, it is described by the following equation:

$$q = \frac{cP_{\text{beam}}}{wlh} \quad (4)$$

In order to reach the desired solution, the boundary conditions, listed in Table 1 were set.

The simulations show that, provided the beam is powerful enough and focused on a small area, the heated region has a significantly higher temperature than room temperature. For instance, typical simulations results are shown on Fig. 2. Another important observation is that the temperature rapidly drops outside the heated region, which is crucial for the implementation of zone-melting recrystallization (ZMR) [8].

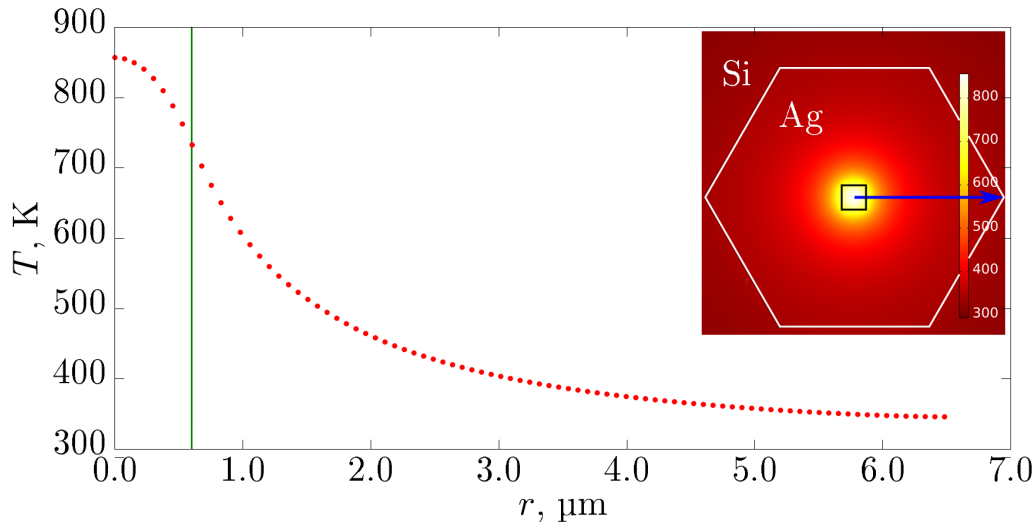


Fig. 2. Line profile of the temperature across the surface of the Ag microparticle (the parameters of the simulation are $l = w = 1.2 \mu\text{m}$, $h = 300 \text{ nm}$, $P_{\text{beam}} = 0.54 \text{ W}$). The green line indicates the boundary between the heated and non-heated region. Inset: Colour map of the temperature. The blue arrow corresponds to the x-axis of the figure.

EXPERIMENTAL SETUP AND RESULTS

The experiments were performed in SEM Hitachi S-570, modified to acquire digital images [9].

Table 2. Specifications of SEM Hitachi S-570

Accelerating voltage	3–30 kV
Electrons source	Tungsten filament
Max. beam current	300 μA
Magnification	20 \times –100000 \times
Objective aperture	4 holes with different sizes, additional setting with no aperture
Detectors	– Upper in-lens SE detector – Lower SE detector – Measurement of the current through the specimen is possible

Some of the characteristics of the microscope are listed in Table 2. All of the experiments involving high beam current were performed without an aperture. The beam current was controlled by changing the settings of the two condenser lenses. The current through the coils of each condenser lens can be regulated by corresponding knobs (with positions, labeled from 1 to 10, 1 corresponding to the lowest current, therefore longest focal length). By modifying of the focal length of each condenser lens, the image of the filament moves in respect to the condenser apertures, resulting a different amount of electrons passing through the condenser apertures. The electron beam current has been measured using Keith-

ley 617 electrometer. Under normal working conditions for imaging (both condensers knobs set to position 6), the beam current measures up to $I_0 = 5.5 \text{ nA}$ at $U = 28 \text{ kV}$. When both of the condensers are set to their largest focal distance (position 1), the beam current is maximal: $I_{\text{max}} = 18400 \text{ nA} \approx 3300I_0$. The beam current was measured at multiple combinations of condenser lens settings and accelerating voltages. Its highest beam power was

$$P_{\text{beam, max}} = 28 \text{ kV} \times 18 \mu\text{A} = 0.5 \text{ W} \quad (5)$$

When the microscope is working at a high beam current, the secondary electrons signal increases drastically. Degradation of the image quality was observed, due to saturation of the scintillator detector and/or photomultiplier. A special remotely-controlled screen (Fig. 3) was constructed to protect the secondary detector in the subsequent experiments.

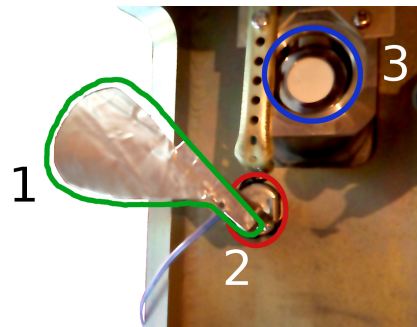


Fig. 3. Protective screen for the SE detector. 1 – aluminum screen, 2 – electric motor, 3 – SE detector.

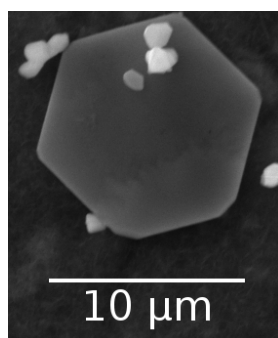


Fig. 4. Silver hexagonal microplate, used in the electron-beam heating experiments.

The micro objects used in the experiments are chemically synthesized silver hexagonal microplates [10]. Their diameter varies between 5–20 μm and their thickness: 200–300 nm. A typical example is shown on Fig. 4.

The goal of these preliminary experiments is to attempt melting of these microplates. If they can be successfully melted, then the beam is powerful enough and after series of further refinements of the experimental setup, the temperature could be set precisely enough for actual annealing.

Results – electron-beam heating

When only electron-beam heating was used, melting was observed at only one configuration of the microscope – the one, giving highest beam power: $U = 30$ kV, both condensers knobs set to 1 (maximal beam current), no objective aperture. One of the successful attempts is shown on Fig. 5. Despite the multiple attempts to melt the particles at lower beam powers, there was no success.

In conclusion, melting of the silver microplates is possible, but only at the beam power set to the maximum possible. In this case, fine tuning of the settings is a challenging task. Furthermore, the resolution of the microscope at these extreme settings is significantly worse, which is an additional complication.

Results – heating by a tungsten filament

These experiments are a preliminary step to the realization of combined heating. The Ag hexagonal microplates were placed on top of a tungsten filament, extracted from a 6 V light bulb (shown on Fig. 6) and then put into the specimen chamber of SEM. The voltage U_{filament} , applied to the filament was gradually increased until melting of the microplates was observed.

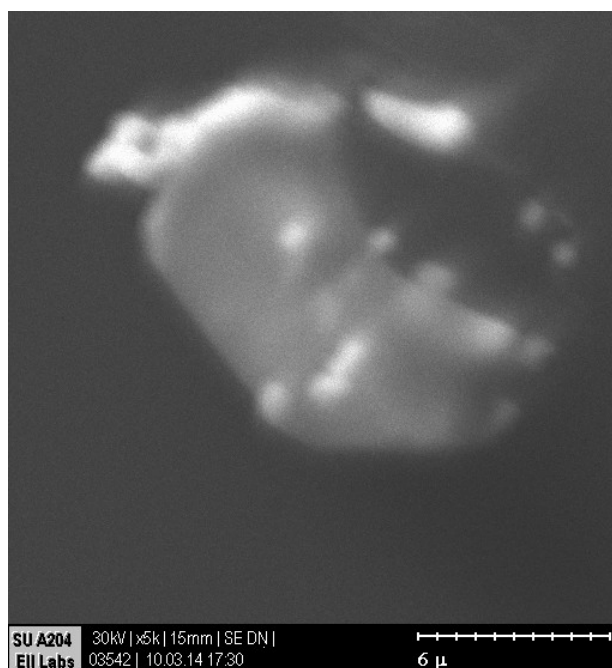
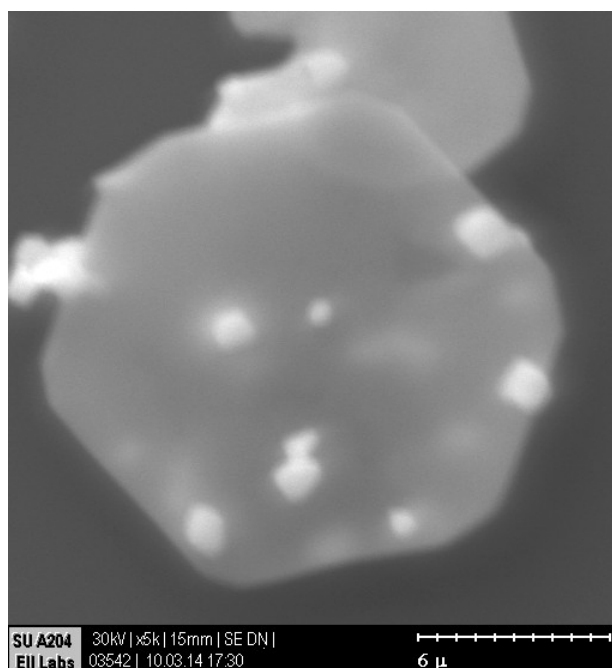


Fig. 5. A successful melting of silver microplates. $U = 30$ kV, both condensers set to 1 (maximal current).

It is worth to mention that the temperature of the filament varies across its length. Typically, it's hottest at the center and cooler at the ends since the copper wires act as a heat sink. A consequence of this is the fact that according to their location, the Ag microplates begin to melt at different filament voltages. More observations are listed in Table 3.

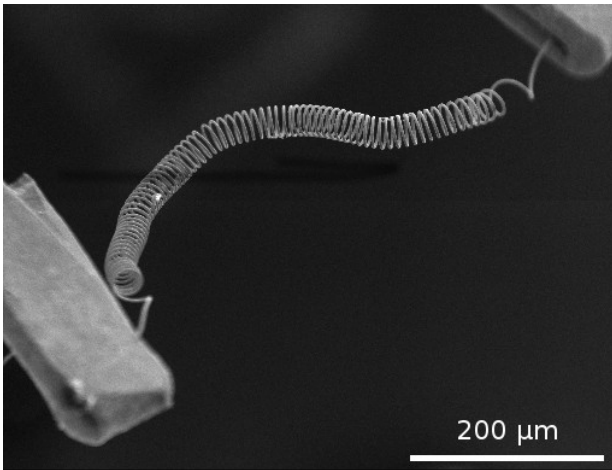


Fig. 6. Tungsten filament, used as a heater

Table 3. Results from the preliminary filament-only heating

Filament voltage	Observations
1.5 V	Particle A near the center of the filament start to melt slowly (Fig. 7, top). Particle B near the center, attached lightly to the filament shows weak signs of melting (Fig. 7, bottom).
2 V	Particle B starts rapid evaporation (Fig. 7, bottom-right).
4 V	Formation of Ag microspheres is observed (Fig. 7, left)
6 V	At the ends of the filament, there are still unaffected silver hexagonal microparticles (Fig. 7, right).

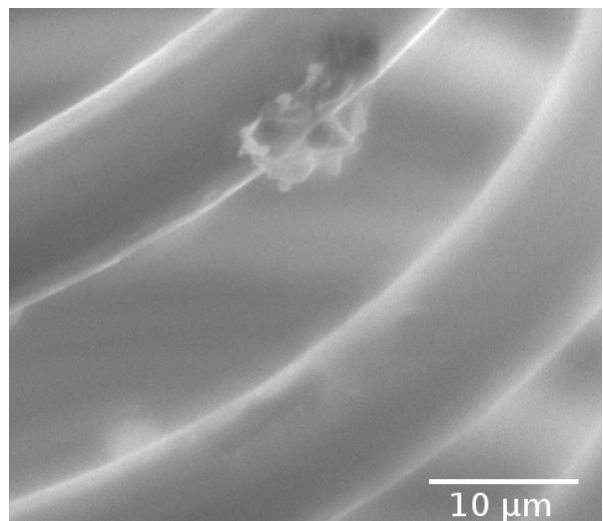
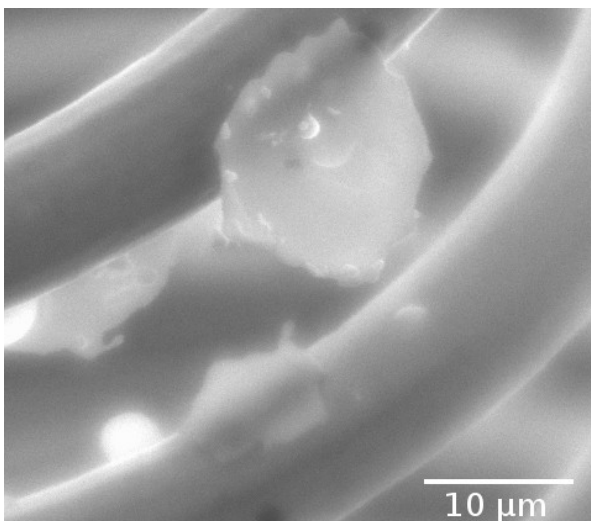
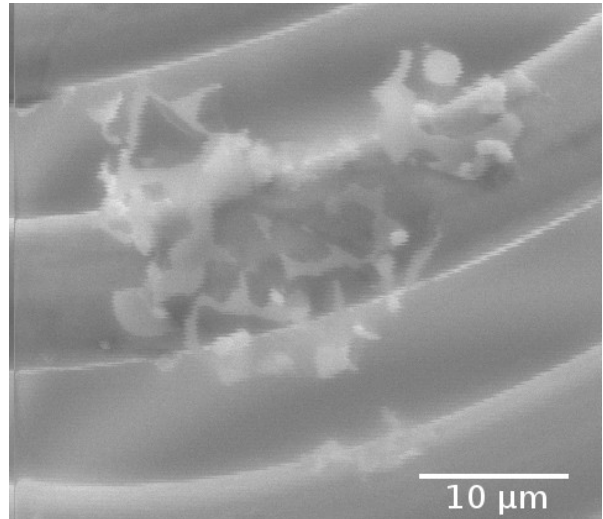
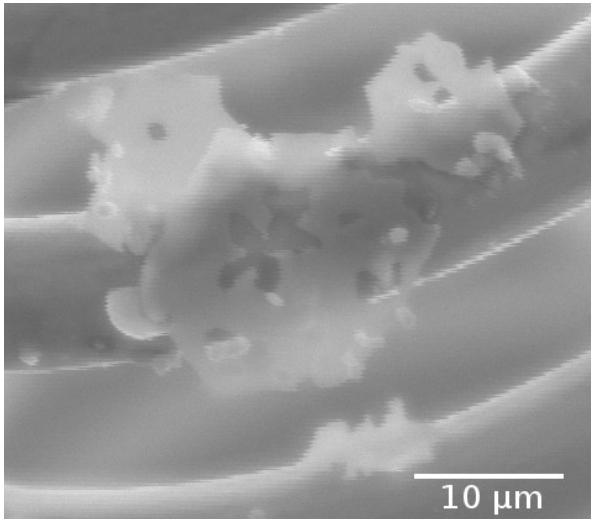


Fig. 7. Top: Particle A at two different moments of melting at $U_{\text{filament}} = 1.5$ V. Bottom: Particle B starts rapid melting at $U_{\text{filament}} = 2$ V.

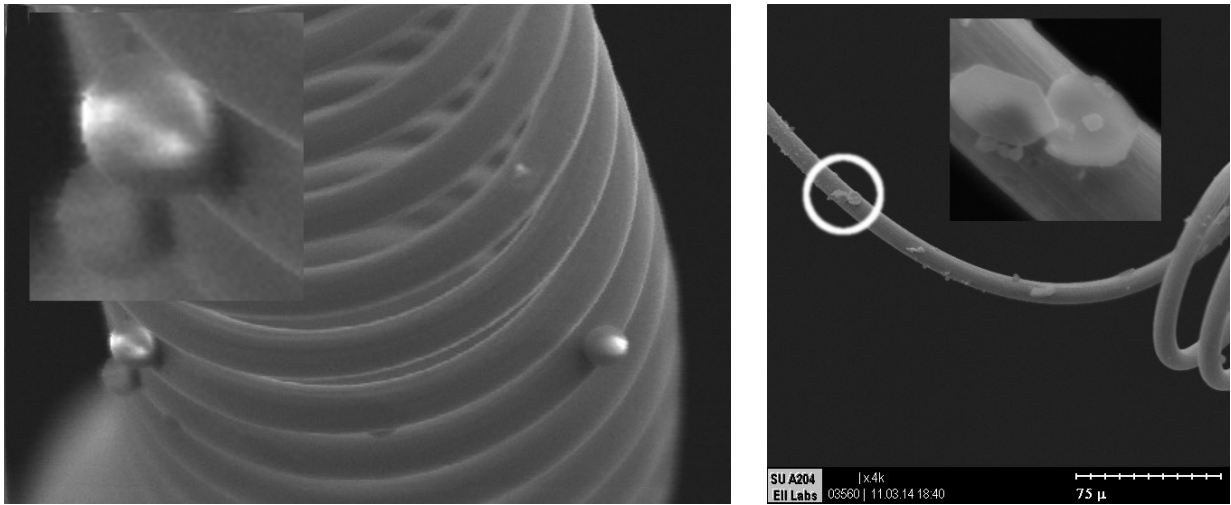


Fig. 8. Left: Silver microspheres at 4 V. Right: Even after heating at 6 V, the particles near the ends of the filament remain unaffected.

Results – combined heating

The combined heating method is proposed to overcome the flaws of the electron-beam only heating. Again, a tungsten filament is used as a heater. It preheats the silver microparticle and less beam power is needed to melt it.

The condenser knobs were both set to 3 (providing less than the maximum beam current, but still noticeably higher, compared to imaging regime). The

voltage, applied to the heating filament was gradually increased until melting of the observed microplates started at $U_{\text{filament}} = 0.8 \text{ V}$ (see Fig. 9).

Compared to the previous experiments, the combined heating method needs much less beam power (6.6 mW vs 540 mW in the case of electron-beam heating) and lower filament voltage (0.8 V vs 1.5 V). This method allows finer control of the heating power, while keeping the SEM resolution good enough.

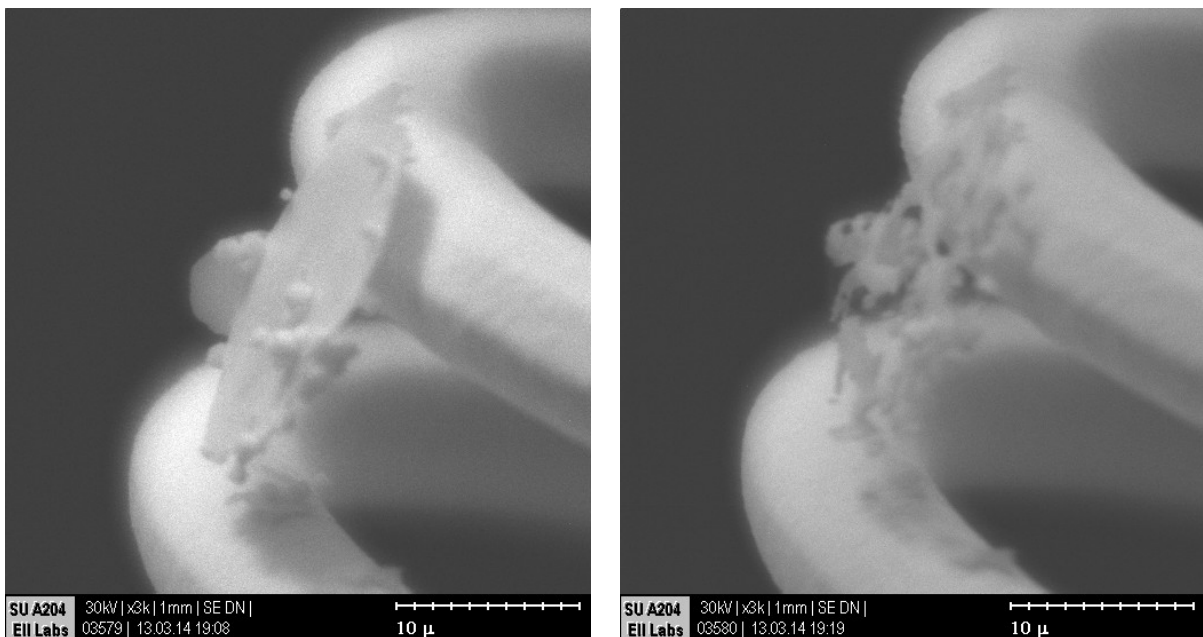


Fig. 9. A successful melting of silver microplates, using both electron-beam heating and filament heating.

CONCLUSIONS

It was shown (both by simulations and by experiments) that it is possible to melt silver microparticles by heating them with electron beam in SEM. Successful melting experiments were only performed when the beam power was set to maximum. To overcome this, a more appropriate setup for precise control of the heating process was proposed, combining electron-beam heating and tungsten filament heater. After further improvements of the setup, it has the potential to be used for zone-melting recrystallization of micro objects. As a side result, spherical Ag microparticles were obtained.

REFERENCES

- [1] R. F. Egerton, *Physical Principles of Electron Microscopy*, Springer US, Boston, MA (2005); <http://www.springerlink.com/index/10.1007/b136495>
- [2] P.J. Goodhew, J. Humphreys, R. Beanland, *Electron Microscopy and Analysis, Third Edition*, CRC Press (2000); <http://www.crcpress.com/product/isbn/9780748409686>
- [3] Z. L. Wang, *Scanning Microscopy for Nanotechnology*, Springer New York, New York, NY (2006); <http://www.springerlink.com/index/10.1007/978-0-387-39620-0>
- [4] S. Reed, *Electron microprobe analysis and scanning electron microscopy in geology*, Cambridge University Press (2005); http://bilder.buecher.de/zusatz/14/14770/14770790_vorw_1.pdf
- [5] A. T. Fiory, "Methods in rapid thermal annealing" in *Proceedings of RTP 2000, Eighth International Conference on Advanced Thermal Processing of Semiconductors* (2000) pp. 15–25.
- [6] F.P. Incropera, *Fundamentals of heat and mass transfer*, Sixth edition, John Wiley & Sons (2011).
- [7] D. Drouin, A.R. Couture, D. Joly, X. Tastet, V. Aimez, R. Gauvin, *Scanning* **29**, 92–101 (2007).
- [8] T. Kieliba, "Zone-Melting Recrystallization for Crystalline Silicon Thin-Film Solar Cells", Ph.D. Thesis (2006).
- [9] S. Russev, G. Tsutsumanova, S. Angelov, K. Bachev, *J. Microsc.* **226**, 64–70 (2007).
- [10] D. L. Lyutov, K. V. Genkov, A. D. Ziapkov, G. G. Tsutsumanova, A. N. Tzonev, L. G. Lyutov, S. C. Russev, *Mater. Chem. Phys.* **143**, 642–646 (2014).

ЕЛЕКТРОННО-ЛЪЧЕВО ОТГРЯВАНЕ НА МИКРООБЕКТИ И СТРУКТУРИ В SEM

К. Генков, Г. Цуцуманова, Ст. Хаджийски, А. Цонев, Д. Лютов, Ст. Русев

Физически факултет, Софийски университет "Св. Климент Охридски",
ул. "Джеймс Баучер" №5, 1164 София, България

(Резюме)

Целта на тази работа е да провери възможностите за използване на фокусиран електронен сноп в сканиращ електронен микроскоп (SEM) за прецизно отгряване на обекти и структури с микронни размери. Освен наблюдаването на вторични електрони, обратно разсеяни електрони, рентгеново лъчение, при взаимодействието на ускорения електронен сноп със сканираната повърхност се наблюдава и отдаване на енергия по повърхността ѝ. Това позволява при големи токове на електронния сноп, SEM да бъде използван за отгряване на микрообекти и структури.

Възможни приложения на този метод са подобряването на кристалната структура чрез зонно отгряване, премахването на дефекти или нежелани микрообекти, микрозапояване, получаване на нови микрообекти (например със сферична форма) и други. Възможността за получаване на микрокристали с идеална кристална структура чрез зонно отгряване позволява подготовянето на подходящи златни и сребърни образци с приложение в плазмониката.